Published in final edited form as:
Mol Cancer Ther. 2010 May ; 9(5): 1298–1307. doi:10.1158/1535-7163.MCT-09-0707.

Inhibition of Mer and Axl Receptor Tyrosine Kinases in Astrocytoma Cells Leads to Increased Apoptosis and Improved Chemosensitivity

Amy K. Keating[1], **Grace K. Kim**[1], **Ashley E. Jones**[1], **Andrew M. Donson**[1], **Kathryn Ware**[1], **Jean M. Mulcahy**[2], **Dana B. Salzberg**[1,4], **Nicholas K. Foreman**[1], **Xiayuan Liang**[3], **Andrew Thorburn**[2], and **Douglas K. Graham**[1]

[1] Department of Pediatrics, School of Medicine, University of Colorado Denver, Aurora, Colorado

[2] Department of Pharmacology, School of Medicine, University of Colorado Denver, Aurora, Colorado

[3] Department of Pathology, School of Medicine, University of Colorado Denver, Aurora, Colorado

[4] Phoenix Children's Hospital, Phoenix, Arizona

Abstract

Astrocytomas account for the majority of malignant brain tumors diagnosed in both adult and pediatric patients. The therapies available to treat these neoplasms are limited, and the prognosis associated with high-grade lesions is extremely poor. Mer (MerTK) and Axl receptor tyrosine kinases (RTK) are expressed at abnormally high levels in a variety of malignancies, and these receptors are known to activate strong antiapoptotic signaling pathways that promote oncogenesis. In this study, we found that Mer and Axl mRNA transcript and protein expression were elevated in astrocytic patient samples and cell lines. shRNA-mediated knockdown of Mer and Axl RTK expression led to an increase in apoptosis in astrocytoma cells. Apoptotic signaling pathways including Akt and extracellular signal–regulated kinase 1/2, which have been shown to be activated in resistant astrocytomas, were downregulated with Mer and Axl inhibition whereas poly(ADP-ribose) poly-merase cleavage was increased. Furthermore, Mer and Axl shRNA knockdown led to a profound decrease of astrocytoma cell proliferation in soft agar and a significant increase in chemosensitivity in response to temozolomide, carboplatin, and vincristine treatment. Our results suggest Mer and Axl RTK inhibition as a novel method to improve apoptotic response and chemosensitivity in astrocytoma and provide support for these oncogenes as attractive biological targets for astrocytoma drug development.

Introduction

Astrocytomas are the most common brain tumor diagnosed in adults and children. The prognosis associated with high-grade astrocytomas is especially poor and treatment options are limited. Current standard of care consists of local control with surgical resection and radiation, which is difficult given the diffuse and invasive nature of the tumor, followed by

Corresponding Author: Amy K. Keating, Department of Pediatrics, University of Colorado Denver, Mail Stop 8302, Room P18-4105, 12800 East 19th Avenue, Aurora, CO 80045. Phone: 303-724-4027; Fax: 303-724-4015. Amy.Keating@UCDenver.edu.

Note: Supplementary material for this article is available at Molecular Cancer Therapeutics Online (http://mct.aacrjournals.org/).

Disclosure of Potential Conflicts of Interest
No potential conflicts of interest were disclosed.

treatment with temozolomide. This standard therapy results in a median survival of 14.6 months with only 26.5% of patients surviving to 2 years (1, 2). Additionally, there is a large potential for morbidity associated with the current available therapies, and surgical treatments needed for even low-grade tumors may result in significant neurologic deficits (3). Furthermore, astrocytic tumors show several key treatment resistance mechanisms, including decreased apoptosis through the phosphatidylinositol 3-kinase (PI3K) and mitogen-activated protein kinase (MAPK) signaling pathways, and upregulation of these pathways is correlated with adverse clinical outcomes (4). There is clearly a need for a more detailed understanding of the molecular mechanisms and pathways involved in astrocytoma to enable the development of novel therapeutic targets and improved treatment options.

Abnormal activation of receptor tyrosine kinases (RTK) has been implicated in the development of cancer through proliferation, apoptosis inhibition, and migration/metastasis. The Mer (MerTK) and Axl RTKs are part of the TAM (*T*yro-3, *A*xl, *M*er) RTK subfamily, and these receptors have been associated with a spectrum of human cancers. Mer was originally cloned from a B lymphoblastoid cDNA library (5) and later from a glioblastoma multiforme cell line (6), whereas Axl was identified as a transforming gene in human myeloid leukemia cells (7). Aberrant expression of Mer and/or Axl has been detected in solid tumors including lung cancer, breast cancer, prostate cancer, rhabdomyosarcoma, kidney cancer, osteosarcoma, ovarian cancer, pancreatic cancer, and uterine cancer. Prognostically, overexpression of Axl was predictive of higher rates of metastasis and inferior outcomes in osteosarcoma, acute myeloid leukemia, lung cancer, and pancreatic cancer (8–11), whereas coexpression of Mer and Axl has been linked with poor prognosis in gastric carcinoma (12).

Recent reports have also confirmed overexpression of Axl in astrocytoma/glioblastoma (13, 14). However, the functional consequences of Axl expression in astrocytoma related to signaling, cell survival, and proliferation are poorly understood. Furthermore, a role for the Mer RTK in astrocytoma has previously been unrecognized. In this study, we report abnormal expression of Mer and Axl RTKs in astrocytoma cell lines and primary patient samples. Inhibition of either Mer or Axl RTK expression led to a profoundly different phenotype compared with the parental astrocytic cells, with increased apoptosis and apoptotic signaling, decreased growth and proliferation, and higher sensitivity to chemotherapeutic agents. This report elucidates the role of Mer and Axl RTKs in astrocytoma growth and resistance to chemotherapy and provides support for these proteins as attractive novel therapeutic targets.

Materials and Methods

Brain tissue samples

Normal brain tissue was obtained from autopsy samples at the University of Colorado Hospital. Central nervous system (CNS) tumor samples were obtained from patients that presented for treatment at The Children’s Hospital and the University of Colorado Hospital between 1995 and 2007. All studies were conducted in compliance with institutional human subjects protection review board regulations. Tumors were classified by clinical neuropathologists according to WHO histologic tumor classification.

Microarray analysis

The analysis included 85 tumor specimens, 32 of which were astrocytoma patient samples. In the astrocytoma patient sample group, there were 7 *de novo* pediatric glioblastoma, 6 pediatric radiation-induced glioblastoma, 3 adult glioblastoma, 3 pilomyxoid astrocytoma, 5 pilocytic astrocytoma, 1 ganglioglioma, 1 pleomorphic xanthoastrocytoma, 1 anaplastic

astrocytoma, and 5 miscellaneous high-grade gliomas. Nonastrocytic tumors included 17 ependymoma, 9 medulloblastoma, 5 atypical teratoid/rhabdoid tumors, 2 choroid plexus papillomas, 1 choroid plexus carcinoma, 14 pediatric sarcomas (including 8 rhabdomyosarcomas), and 5 meningiomas. One specimen of normal pediatric choroid plexus was also included in the evaluation. RNA was extracted from specimens and hybridized to Affymetrix HG-U113 plus 2 microarray chips (Affymetrix) according to the manufacturer's instructions as previously described (15). Data were exported to GeneSpring GX 7.3.1 bioinformatics software (Silicon Genetics) and analyzed by standard technique as previously reported (15). Gene expression values for *MERTK* (Affymetrix probe set 206028), *AXL* (202686), *GAS6* (202177), and *TYRO-3* (211431 and 211432), measured as normalized hybridization intensity, were obtained and used for correlation analysis using GraphPad Prism (v. 4.0.3).

Cell lines

The U251, U118, T98G, and A172 cell lines were obtained from American Type Culture Collection and maintained per culture guidelines. D3, D19, and G12 cell lines were derived from glioblastoma multiforme patient samples as previously described (16).

Immunoblotting of Mer and Axl RTKs and downstream apoptotic signals

Lysates were prepared from cells or homogenized tumor samples using a lysis buffer containing 50 mmol/L HEPES (pH 7.5), 150 mmol/L NaCl, 10 mmol/L EDTA, 10% (v/v) glycerol, 1% (v/v) Triton X-100, 1 mmol/L sodium orthovanadate, 0.1 mmol/L sodium molybdate, and protease inhibitors (Roche). Lysates were placed on ice for 10 minutes, and protein supernatant was collected by centrifugation. Cell lysates were resolved on SDS-PAGE gels and transferred onto nitrocellulose membranes. Membranes were blocked in a buffer of TBS with Tween 20 containing 5% milk. The immunoblots were probed with the following antibodies at concentrations recommended by the manufacturers' protocols: human Mer (monoclonal antibody A311, Caveo Therapeutics; refs. 17, 18); human Axl (R&D Systems); phospho-AKT (Ser473), AKT, phospho-extracellular signal–regulated kinase (Erk)-1/2 (Thr202/Tyr204), Erk1/2, and poly(ADP-ribose) polymerase (Cell Signaling Technologies); and actin goat polyclonal (Santa Cruz Biotechnology). Proteins were visualized by horseradish peroxidase chemiluminescence detection (Perkin-Elmer). In cases where a single actin protein loading control is shown, a single membrane was run, stripped, and reprobed for the second and further proteins. All immunoblots are representative of a minimum of three independent experiments.

Production of shRNA clones

Lentiviral vectors (pLKO.1) containing shRNA sequences targeting Mer (shMer1, oligo ID: TRCN0000000862 and shMer4, oligo ID: TRCN0000000865), Axl (shAxl8, oligo ID: TRCN0000000574 and shAxl9, oligo ID: TRCN0000000575), or nonsilencing control green fluorescent protein (GFP; shControl) were obtained from Open Biosystems. Replication-incompetent viral particles were generated using the 293FT cell line and the third-generation packaging system (two packaging plasmids and one envelope plasmid) developed by the laboratory of Dr. Didier Trono. Cell infection and puromycin selection were done according to previous descriptions (19). Puromycin--resistant colonies were typically observed on days 9 to 13. Stable, clonal lines were developed from heterogenous Mer and Axl shRNA knockdown cell populations by single-cell flow cytometry sorting for low Mer or Axl expression.

Functional assay of apoptosis

G12 control cells (shControl) and knockdown cells (shMer1 and shAxl9) were plated in RPMI containing 10% fetal bovine serum (FBS) at 60% to 70% confluence and allowed to adhere. The medium was removed from all plates and replaced with RPMI/FBS in the fed group or with RPMI only in the 24-hour serum starvation group. Twenty-four hours later, cells were lifted after treatment with 0.02% EDTA in PBS, then stained for 20 minutes with 1 μmol/L Yo-Pro-1 iodide and 1.5 μmol/L propidium iodide (PI; Invitrogen) in PBS and analyzed by flow cytometry.

Autophagy analysis

G12 control cells (shControl) and knockdown cells (shMer1 and shAxl9) were plated at 750,000 cells per well in four wells each of a six-well plate in RPMI medium containing 10% FBS and 1% penicillin-streptomycin and allowed to adhere overnight. Medium was removed and cells were washed with PBS and treated with one of four conditions: RPMI/FBS without lysosomal protease inhibitors (control: DMSO, 0.4 μL/mL; methanol, 2 μL/mL), RPMI/FBS with lysosomal protease inhibitors (pepstatin A, 0.4 μL/mL; E64D, 2 μL/mL), Earle's balanced salt solution without inhibitors, and Earle's balanced salt solution with inhibitors. Cells were incubated for 4 hours and then removed from the incubator on ice. Whole-cell lysates were prepared using 100 μL of radioimmunoprecipitation assay lysis buffer per well as previously described (20) and then sonicated; protein supernatant was collected by centrifugation. Autophagic flux assays were done by Western blotting for LC3-II formation after Earle's balanced salt solution starvation in the presence or absence of lysosomal pro-tease inhibitors as recommended (20). Polyvinylidene difluoride membranes were blotted with antibodies against LC3 (MBL) and actin (Sigma).

Soft-agar assay

Six-well plates were layered with 1.5 mL of 0.5% Difco Noble Agar (Invitrogen) rehydrated with RPMI/FBS, followed by plating with 1.5 mL of cell lines suspended in 0.4% Noble Agar rehydrated in RPMI/FBS. G12 shControl, shMer, and shAxl cells were plated at a concentration of 100,000 cells per well in triplicate, whereas A172 shControl, shMer, and shAxl cells were plated at a concentration of 25,000 cells per well in triplicate. Cells were incubated for 3 weeks at 37°C and 5% CO_2, stained with nitrotetrazolium blue (1 mg/mL) for 24 hours, and counted in triplicate with the Bio-Rad ChemiDoc XRS Imaging System and Quantity One software (v. 4.6.6). Colony counts of the Mer and Axl shRNA knockdown lines were compared with the control and statistically analyzed with a two-tailed *t* test using GraphPad Prism (v. 4.0.3).

Chemotherapeutic treatment and MTT assay

Standard growth curves for each control and shRNA cell line were used to determine appropriate cell concentration for optimal growth conditions. Analysis of growth curves showed no significant difference in cell lines over the experimental time period. Cell lines were seeded in triplicate at a density of 3,200 cells per well in 96-well tissue culture plates and incubated for 12 to 16 hours at 37°C and 5% CO_2. Chemotherapeutic agents, in various concentrations, were added to the cells and incubated for 48 hours. Control treatments consisted of equal volumes of RPMI or mitomycin C. Cellular metabolic activity was measured at 48 hours with addition of MTT reagent (Sigma-Aldrich) and absorbance was measured at 570 nm. Relative cell number was calculated by subtraction of background absorbance (mitomycin C treated) and normalization to untreated absorbance (RPMI treated). IC_{50} with a 95% confidence interval (95% CI) was generated using GraphPad Prism (v. 4.0.3).

Results

Mer and Axl RTKs are highly expressed in astrocytic tumor patient samples and cell lines

Microarray evaluation of mRNA transcript levels was done on 85 brain and solid tumor samples of a variety of histologic subtypes. In the studied tumors, there was detectable expression of Mer and Axl, as well as their common ligand Gas6. High Gas6 expression was independently correlated with both high Mer expression (Pearson $r = 0.32$, $P = 0.003$; Supplementary Fig. S1A) and high Axl expression (Pearson $r = 0.57$, $P < 0.0001$; Supplementary Fig. S1B). High coexpression of Mer and Axl was also detected in the brain tumor samples (Supplementary Fig. S1C) with a Pearson $r = 0.49$ ($P < 0.0001$). The expression pattern of the third TAM family member, Tyro-3, was also evaluated and showed that increased Tyro-3 expression was not significantly correlated with Mer, Axl, or Gas6 expression (data not shown).

Each individual histologic subset was also evaluated for the expression patterns of TAM family receptors and their ligands. The levels of highest coexpression were in the subset of astrocytic tumors, where Mer and Axl coexpression was highly correlated (Fig. 1A), with a Pearson $r = 0.79$ ($P < 0.0001$). In contrast to the large combined brain tumor group, Gas6 correlation with Mer and Axl could not be shown in astrocytic tumors due to the smaller number of patients included in the analysis. These data are consistent with and expand on previous reports of elevated Axl protein expression in astrocytic brain tumors (13, 14), and represent the first report of Mer overexpression in these tumors as well as the coexpression of Mer and Axl RTKs.

Follow-up immunoblot analysis for Mer and Axl protein expression was done on astrocytic patient tumor samples, and high levels of Mer and Axl RTKs were found in low-grade astrocytic and high-grade astrocytic tumors (Fig. 1B). A total of 19 patient samples were evaluated, 18 of which expressed Mer, 18 of which expressed Axl, and 17 of which coexpressed Mer and Axl. A difference in size and number of Mer RTK bands may represent differential glycosylation of the extracellular domain of Mer, resulting in multiple glycoforms.

An evaluation of seven glioblastoma cell lines found similar high levels of RTK protein expression. Mer protein was expressed in four lines, whereas Axl protein was found in all of the cell lines tested (Fig. 1C). The G12 and A172 cell lines were chosen for further investigations as they contained moderate and large degrees of Mer and Axl RTK protein expression, respectively.

Inhibition of Mer or Axl receptor expression with transduction of shRNA

We introduced stable shRNA constructs designed to inhibit the transcription of Mer, Axl, and GFP (shControl) into two astrocytoma cell lines, G12 and A172. shGFP was chosen as the control, as it uses the experimental vector and engages the siRNA machinery without silencing any human gene. Two different Axl shRNA constructs (shAxl8 and shAxl9) were transduced into the G12 and A172 astrocytoma cell lines. Although two Mer shRNA constructs (shMer1 and shMer4) were introduced into the G12 cell line, only one shMer construct (shMer1) was successfully integrated into the A172 line, likely due to the poor growth phenotype associated with Mer knockdown in this cell line. Therefore, two independent A172 shMer1 clones (shMer1A and shMer1B) were included in further studies of the A172 line.

Immunoblot analysis of the shRNA clones showed significant knockdown of Mer and Axl expression in both the G12 (Fig. 2A) and the A172 lines (Fig. 2B). Mer expression relative to control was moderately inhibited in G12 shMer1 and shMer4 cells and more significantly

in A172 shMer1A and shMer1B cells, whereas Axl expression levels relative to control showed that G12 and A172 shAxl clones had profound inhibition of expression. The expression of Mer and Axl in the shControl and parental lines was comparable, and knockdown of either Mer or Axl did not affect protein levels of the other RTKs (data not shown and Fig. 3B).

Inhibition of Mer and Axl RTKs leads to increased apoptosis and autophagy

The effect of Mer and Axl knockdown on astrocytoma cell survival was evaluated in a flow cytometric assay using Yo-Pro/PI staining to detect apoptosis. Yo-Pro will stain cells with a disrupted plasma membrane, as is present during early and late apoptosis, whereas PI requires membrane rupture, and cells will show positive staining with late apoptosis and necrosis. The survival phenotype of G12 cells with Mer or Axl knockdown was remarkably different from that of control cells. shControl cells had less than 1% apoptosis with or without the presence of serum. Inhibition of Mer or Axl led to increased apoptosis in response to serum starvation, with Mer knockdown leading to 5.57% apoptotic cells and Axl knockdown leading to 26.96% apoptotic cells (Fig. 3A).

The apoptotic phenotype from Mer and Axl inhibition was further delineated with immunoblot analysis of apoptotic signaling pathways in G12 and A172 knockdown lines. In the two cell lines, shControl cells both under normal culture conditions and with serum starvation had easily detectable p-Akt and p-Erk1/2, indicating that antiapoptotic survival pathways were activated. In comparison, G12 and A172 shMer and shAxl knockdown cells had a reduced amount of p-Akt and p-Erk1/2, indicating prosurvival pathway activation was decreased (Fig. 3B and Supplementary Fig. S2), suggesting a possible mechanism for the decreased survival when the cells were stressed by serum starvation. Of note, activation of Akt was more prominent in the astrocytoma cells grown in media containing serum, which contains the TAM RTK ligand Gas6, than in those grown under conditions of starvation. It is possible that the fed cells had some limited activation of this pathway through the partner RTK that was not knocked down; however, the pathway activation was still well below that of the control lines and was not reiterated by Erk pathway activation in both lines (Fig. 3B and Supplementary Fig. S2). Additionally, the increased poly(ADP-ribose) polymerase cleavage in the Mer and Axl knockdown cell lines, particularly under conditions of serum starvation, was consistent with the decreased cellular survival of these lines (Fig. 3B).

The effect of Mer and Axl knockdown on astrocytoma cell autophagy was also evaluated. During active autophagy, microtubule-associated protein light chain 3 (LC3) is converted from its cytosolic form LC3-I to LC3-II, indicating upregulation of autophagy (20). Treatment with lysosomal protease inhibitors, pepstatin A and E64D, stabilizes LC3-II, allowing one to discriminate between increased autophagic flux and decreased fusion with the lysosome. At baseline and with serum starvation stress, shControl cells exhibit only a minimal amount of autophagy. In contrast, astrocytoma cells with Mer or Axl RTK inhibition show a large increase in autophagic flux, and this increase in autophagy is present even without the stress of serum starvation.

Inhibition of Mer or Axl results in decreased nonadherent colony formation

To assess the effect of Mer and Axl inhibition on long-term cellular colony formation potential, control and knockdown shMer and shAxl clones were plated in soft agar for 3 weeks. In both G12 and A172 lines, knockdown of either Mer or Axl led to significantly decreased colony formation compared with the control. In the G12 line, Mer inhibition led to growth that was less than 5% of control (shMer1 $P = 0.0008$, shMer4 $P < 0.0001$), whereas Axl inhibition led to growth that was less than 10% of control (shAxl8 $P = 0.0005$, shAxl9 $P = 0.0008$; Fig. 4A). In the A172 line, Mer inhibition led to growth that was less

than 25% of control (shMer1A $P = 0.006$, shMer1B $P = 0.005$), whereas Axl inhibition led to growth that was less than 30% of control (shAxl8 $P = 0.03$, shAxl9 $P = 0.003$; Fig. 4B). There was no statistical difference in soft-agar growth between the Mer and Axl shRNA knockdown lines. Thus, inhibition of either RTK yielded a dramatic decrease in astrocytoma cell colony formation, and the presence of Mer or Axl alone could not compensate for the loss of the other tyrosine kinase receptor.

Inhibition of Mer or Axl significantly increases chemo-sensitivity

To further evaluate the survival response mediated by Mer and Axl in astrocytoma cells, control and knockdown lines were treated with the chemotherapeutic agents to induce an apoptotic response. Multiple chemotherapeutic agents known to have clinical efficacy in the treatment of brain tumors (temozolomide, carboplatin, and vincristine) were tested at clinically attainable concentration ranges. The IC_{50}, the drug concentration at which 50% of the cells are no longer metabolically active, and the 95% CI for the IC_{50} were calculated. Treatment of G12 cells with temozolomide revealed that either Mer or Axl knockdown significantly decreased the IC_{50} from 68.6 μmol/L to a range of 1 to 18.2 μmol/L (Fig. 5A). Treatment of A172 cells with carboplatin showed that this astrocytoma line was completely resistant to carboplatin treatment, even at concentrations as high as 64 μmol/L. However, Mer or Axl inhibition caused the cells to become susceptible to carboplatin with IC_{50} concentrations of 0.035 to 0.82 μmol/L (Fig. 5B). In all cases, cells with Mer inhibition were significantly more chemo-sensitive than control cells, and in most cases, cells with Axl inhibition were also more significantly chemosensitive (Table 1). The only exceptions to the improved chemosensitivity offered by Mer or Axl knockdown were the shAxl9 construct in G12 cells treated with carboplatin and the shAxl9 A172 cells treated with temozolomide or vincristine. In these cases, however, most of the IC_{50} values showed a trend toward improved chemosensitivity, and in the case of the G12 shAxl9 cells treated with carboplatin, the knockdown cells were much more sensitive than controls; however, the confidence interval was too large to show this difference with statistical significance.

Discussion

Astrocytic tumors are typically only minimally responsive to current chemotherapeutic agents, and clinical treatment has relied on the success of surgical resection to ensure progression-free survival. The recent addition of temozolomide to treatment regimens has extended median survival times for the disease, but only from 12 to 15 months (1). Identification of new treatment strategies is needed for patients with high-grade, inoperable, or progressive tumors. In this study, we provide data to support the consideration of Mer and Axl RTK inhibition as a novel therapeutic approach to astrocytoma treatment.

The normal expression patterns of Mer and Axl in brain have been previously explored by several groups. Prieto et al. have studied the expression of Mer and Axl in the developing rat brain and have found that the common ligand Gas6 is expressed throughout the CNS whereas Mer and Axl have limited expression at the mRNA and protein levels (21). Recently, Cahoy et al. have evaluated CNS cell subtypes in the mouse and have reported that Mer, Axl, and Gas6 mRNAs are all expressed in the murine astrocyte. Other subsets including murine neurons and oligodendrocytes have very little Mer and Axl expression (22), except for limited temporal expression in hypothalamic GnRH neurons (23). Initial reports on the cloning of human Mer and the expression patterns in humans found minimal detectable transcript levels of Mer in whole-brain preparation (5). Hutterer et al. have reported that Axl expression is absent in nonneoplastic brain (13). In contrast, by microarray we found increased Mer and Axl in astrocytoma patient samples and that there was a significant correlation between Mer and Axl expression (Fig. 1A). Furthermore, an increased expression of Gas6 was associated with increased Mer/Axl expression in the

patient samples, suggesting the possibility of autocrine or paracrine activation of the Mer/Axl oncogenes in astrocytoma.

Expression of Mer and/or Axl has been previously reported in a variety of malignancies (24), including Axl expression in gliomatous tumors (13), but most reports did not investigate the coexpression of Mer and Axl in the cancer subtypes. In one report in which Mer and Axl expression were evaluated, the coexpression of these RTKs in gastric carcinoma was associated with a significantly poorer outcome compared with patients who expressed either RTK alone (12). These data, coupled with our findings of increased Mer and Axl expression in astrocytoma patients and that inhibition of either of these RTKs yields a significant decrease in astrocytoma survival/growth, suggest that there may be an interdependence of these related receptors in some cancer subtypes. An analysis of Mer and Axl functions in normal cell types, including platelets and natural killer cells, also supports this hypothesis. For example, in platelets, all three TAM family receptors are expressed and the targeted knockout of any single receptor yields the phenotype of diminished platelet aggregation and clot stability (25, 26). Furthermore, knockout of one TAM receptor leads to decreased protein expression of the other receptors in the subfamily. This phenomenon was not seen in our astrocytoma investigations. Similarly, loss of any of the three RTKs in natural killer cells compromises cellular maturation and differentiation (27–30). Additional studies will be necessary to more fully understand how these receptors interact or complex in certain cell types or under specific biological conditions.

Mer or Axl inhibition significantly decreased activation of the PI3K and Erk1/2 prosurvival pathways. Previous reports have shown that the PI3K survival pathway is critical for normal CNS cell survival signaling (31, 32). Several groups have published data implicating the PI3K and MAPK pathways in astrocytoma proliferation. Hlobilkova et al. have shown that aberrant activation of Akt is found in both low-grade and high-grade astrocytoma patient samples (33), whereas Mizoguchi et al. showed that the PI3K/Akt and MAPK pathways were abnormally activated in high-grade astrocytomas (34). Interestingly, we found that inhibition of either RTK resulted in a similar phenotype with increased apoptosis and apoptotic biochemical markers as well as decreased astrocytoma cell survival in functional assays.

Our data showed that Mer or Axl inhibition increased the amount of basal and serum starvation associated autophagy considerably. Autophagy is the process of lysosomal degradation wherein the cell digests its own organelles and macromolecules during times of nutrient deprivation or in response to damaged intracellular components (35, 36). Interestingly, autophagy has been implicated in tumor suppression and, somewhat conversely, in chemoresistance. Decreased cellular autophagy resulting from heterozygous *beclin-1* mutation in mice has been associated with high rates of tumor development in mice (37). Along different lines, inhibition of autophagy hastens cell death following chemotherapy treatment (36). Future studies will investigate the role of autophagy in concert with Mer and Axl RTK signaling inhibition and overall survival phenotypes in astrocytoma.

Our findings that either Mer or Axl inhibition leads to decreased prosurvival signaling pathways (Erk1/2, Akt), decreased survival in response to cell stress (serum withdrawal), decreased proliferation in soft-agar assays, and increased chemosensitivity extend the recent observations of Vajkoczy et al. regarding the role of Axl in astrocytoma cell migration and invasion (19). Thus, the Mer/Axl receptors may promote astrocytomas via multiple mechanisms including cell survival, proliferation, and migration. Additionally, our data suggest that targeted inhibition of either Mer or Axl in astrocytoma may be beneficial clinically and may enhance the efficacy of currently used chemotherapeutics. Recent reports of small-molecule inhibitors with efficacy against these receptors (38) make this RTK

subfamily particularly attractive for further study in the treatment of astrocytoma. Additionally, given that Mer and Axl RTKs are ectopically or aberrantly overexpressed in a variety of cancers, the overall potential clinical effect of TAM family inhibition warrants significant further investigations.

Our findings show that Mer and Axl RTKs are highly expressed in astrocytic tumors. We establish that Mer and Axl RTKs regulate antiapoptotic pathway activation and contribute to astrocytoma cell growth and survival *in vitro*. Furthermore, our investigations represent the first report of a profound and significant increase in chemosensitivity in response to standard available chemotherapeutics following RTK inhibition. The cancer-promoting characteristics of the TAM family of RTKs make them attractive therapeutic targets, while inhibition introduces minimal increased therapeutic toxicity. Further *in vivo* studies are needed to determine if Mer and Axl RTK signaling interference, through antibodies and small-molecule kinase inhibitors currently in development, will expand the clinical options available for the treatment of astrocytoma.

Supplementary Material

Refer to Web version on PubMed Central for supplementary material.

Acknowledgments

We thank Deborah DeRyckere, Ph.D., for her insightful comments and collaborations on chemotherapeutic experiments; Rachel Linger, Ph.D., for her technical assistance in the development of the knockdown lines; and Lynn Heasley, Ph.D., for his assistance with the soft-agar assays.

Grant Support

A.K. Keating and J.M. Mulcahy are generously supported by The St. Baldrick's Foundation. A.K. Keating is also supported by The Brent Eley Foundation. D.K. Graham is the Damon Runyon-Novartis Clinical Investigator supported, in part, by the Damon Runyon Cancer Research Foundation (CI-39-07) and is also supported by The Children's Hospital Research Institute.

References

1. Stupp R, Mason WP, van den Bent MJ, et al. Radiotherapy plus concomitant and adjuvant temozolomide for glioblastoma. N Engl J Med. 2005; 352:987–96. [PubMed: 15758009]
2. Stupp R, Hegi ME, Mason WP, et al. Effects of radiotherapy with concomitant and adjuvant temozolomide versus radiotherapy alone on survival in glioblastoma in a randomised phase III study: 5-year analysis of the EORTC-NCIC trial. Lancet Oncol. 2009; 10:459–66. [PubMed: 19269895]
3. Karajannis M, Allen JC, Newcomb EW. Treatment of pediatric brain tumors. J Cell Physiol. 2008; 217:584–9. [PubMed: 18651562]
4. Lefranc F, Rynkowski M, DeWitte O, Kiss R. Present and potential future adjuvant issues in high-grade astrocytic glioma treatment. Adv Tech Stand Neurosurg. 2009; 34:3–35. [PubMed: 19368079]
5. Graham DK, Dawson TL, Mullaney DL, Snodgrass HR, Earp HS. Cloning and mRNA expression analysis of a novel human protooncogene, c-mer. Cell Growth Differ. 1994; 5:647–57. [PubMed: 8086340]
6. Ling L, Kung HJ. Mitogenic signals and transforming potential of Nyk, a newly identified neural cell adhesion molecule-related receptor tyrosine kinase. Mol Cell Biol. 1995; 15:6582–92. [PubMed: 8524223]
7. Liu E, Hjelle B, Bishop JM. Transforming genes in chronic myelogenous leukemia. Proc Natl Acad Sci U S A. 1988; 85:1952–6. [PubMed: 3279421]

8. Nakano T, Tani M, Ishibashi Y, et al. Biological properties and gene expression associated with metastatic potential of human osteosarcoma. Clin Exp Metastasis. 2003; 20:665–74. [PubMed: 14669798]
9. Tsuchiya H, Kanazawa Y, Abdel-Wanis ME, et al. Effect of timing of pulmonary metastases identification on prognosis of patients with osteosarcoma: the Japanese Musculoskeletal Oncology Group study. J Clin Oncol. 2002; 20:3470–7. [PubMed: 12177108]
10. Rochlitz C, Lohri A, Bacchi M, et al. Axl expression is associated with adverse prognosis and with expression of Bcl-2 and CD34 in *de novo* acute myeloid leukemia (AML): results from a multicenter trial of the Swiss Group for Clinical Cancer Research (SAKK). Leukemia. 1999; 13:1352–8. [PubMed: 10482985]
11. Shieh YS, Lai CY, Kao YR, et al. Expression of axl in lung adenocarcinoma and correlation with tumor progression. Neoplasia. 2005; 7:1058–64. [PubMed: 16354588]
12. Wu CW, Li AF, Chi CW, et al. Clinical significance of AXL kinase family in gastric cancer. Anticancer Res. 2002; 22:1071–8. [PubMed: 12168903]
13. Hutterer M, Knyazev P, Abate A, et al. Axl and growth arrest-specific gene 6 are frequently overexpressed in human gliomas and predict poor prognosis in patients with glioblastoma multiforme. Clin Cancer Res. 2008; 14:130–8. [PubMed: 18172262]
14. Vajkoczy P, Knyazev P, Kunkel A, et al. Dominant-negative inhibition of the Axl receptor tyrosine kinase suppresses brain tumor cell growth and invasion and prolongs survival. Proc Natl Acad Sci U S A. 2006; 103:5799–804. [PubMed: 16585512]
15. Addo-Yobo SO, Straessle J, Anwar A, Donson AM, Kleinschmidt-Demasters BK, Foreman NK. Paired overexpression of ErbB3 and Sox10 in pilocytic astrocytoma. J Neuropathol Exp Neurol. 2006; 65:769–75. [PubMed: 16896310]
16. Donson AM, Weil MD, Foreman NK. Tamoxifen radiosensitization in human glioblastoma cell lines. J Neurosurg. 1999; 90:533–6. [PubMed: 10067924]
17. Graham DK, Salzberg DB, Kurtzberg J, et al. Ectopic expression of the protooncogene Mer in pediatric T-cell acute lymphoblastic leukemia. Clin Cancer Res. 2006; 12:2662–9. [PubMed: 16675557]
18. Keating AK, Salzberg DB, Sather S, et al. Lymphoblastic leukemia/lymphoma in mice overexpressing the Mer (MerTK) receptor tyrosine kinase. Oncogene. 2006; 25:6092–100. [PubMed: 16652142]
19. Porter CC, DeGregori J. Interfering RNA-mediated purine analog resistance for *in vitro* and *in vivo* cell selection. Blood. 2008; 112:4466–74. [PubMed: 18587011]
20. Mizushima N, Yoshimori T. How to interpret LC3 immunoblotting. Autophagy. 2007; 3:542–5. [PubMed: 17611390]
21. Prieto AL, Weber JL, Lai C. Expression of the receptor protein-tyrosine kinases Tyro-3, Axl, and mer in the developing rat central nervous system. J Comp Neurol. 2000; 425:295–314. [PubMed: 10954847]
22. Cahoy JD, Emery B, Kaushal A, et al. A transcriptome database for astrocytes, neurons, and oligodendrocytes: a new resource for understanding brain development and function. J Neurosci. 2008; 28:264–78. [PubMed: 18171944]
23. Pierce A, Bliesner B, Xu M, et al. Axl and Tyro3 modulate female reproduction by influencing gonadotropin-releasing hormone neuron survival and migration. Mol Endocrinol. 2008; 22:2481–95. [PubMed: 18787040]
24. Linger RM, Keating AK, Earp HS, Graham DK. TAM receptor tyrosine kinases: biologic functions, signaling, and potential therapeutic targeting in human cancer. Adv Cancer Res. 2008; 100:35–83. [PubMed: 18620092]
25. Angelillo-Scherrer A, de Frutos P, Aparicio C, et al. Deficiency or inhibition of Gas6 causes platelet dysfunction and protects mice against thrombosis. Nat Med. 2001; 7:215–21. [PubMed: 11175853]
26. Angelillo-Scherrer A, Burnier L, Flores N, et al. Role of Gas6 receptors in platelet signaling during thrombus stabilization and implications for antithrombotic therapy. J Clin Invest. 2005; 115:237–46. [PubMed: 15650770]

27. Lemke G, Lu Q. Macrophage regulation by Tyro 3 family receptors. Curr Opin Immunol. 2003; 15:31–6. [PubMed: 12495730]
28. Caraux A, Lu Q, Fernandez N, et al. Natural killer cell differentiation driven by Tyro3 receptor tyrosine kinases. Nat Immunol. 2006; 7:747–54. [PubMed: 16751775]
29. Lemke G, Rothlin CV. Immunobiology of the TAM receptors. Nat Rev Immunol. 2008; 8:327–36. [PubMed: 18421305]
30. Lu Q, Lemke G. Homeostatic regulation of the immune system by receptor tyrosine kinases of the Tyro 3 family. Science. 2001; 293:306–11. [PubMed: 11452127]
31. Shankar SL, O'Guin K, Cammer M, et al. The growth arrest-specific gene product Gas6 promotes the survival of human oligodendrocytes via a phosphatidylinositol 3-kinase-dependent pathway. J Neurosci. 2003; 23:4208–18. [PubMed: 12764109]
32. Shankar SL, O'Guin K, Kim M, et al. Gas6/Axl signaling activates the phosphatidylinositol 3-kinase/Akt1 survival pathway to protect oligodendrocytes from tumor necrosis factor α-induced apoptosis. J Neurosci. 2006; 26:5638–48. [PubMed: 16723520]
33. Hlobilkova A, Ehrmann J, Sedlakova E, et al. Could changes in the regulation of the PI3K/PKB/Akt signaling pathway and cell cycle be involved in astrocytic tumor pathogenesis and progression? Neoplasma. 2007; 54:334–41. [PubMed: 17822324]
34. Mizoguchi M, Betensky RA, Batchelor TT, Bernay DC, Louis DN, Nutt CL. Activation of STAT3, MAPK, and AKT in malignant astrocytic gliomas: correlation with EGFR status, tumor grade, and survival. J Neuropathol Exp Neurol. 2006; 65:1181–8. [PubMed: 17146292]
35. Hotchkiss RS, Strasser A, McDunn JE, Swanson PE. Cell death. N Engl J Med. 2009; 361:1570–83. [PubMed: 19828534]
36. Levine B, Kroemer G. Autophagy in the pathogenesis of disease. Cell. 2008; 132:27–42. [PubMed: 18191218]
37. Liang XH, Jackson S, Seaman M, et al. Induction of autophagy and inhibition of tumorigenesis by beclin 1. Nature. 1999; 402:672–6. [PubMed: 10604474]
38. Li Y, Ye X, Tan C, et al. Axl as a potential therapeutic target in cancer: role of Axl in tumor growth, metastasis and angiogenesis. Oncogene. 2009; 28:3442–55. [PubMed: 19633687]

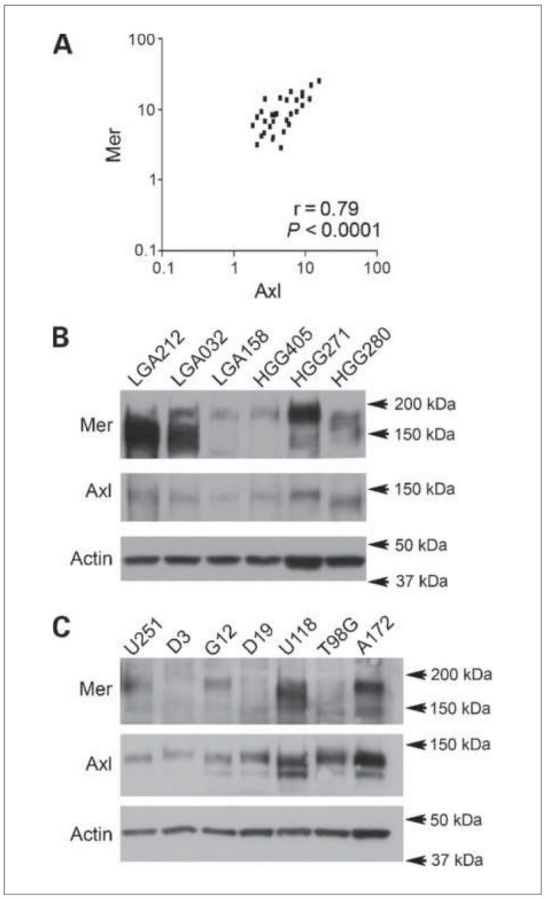

Figure 1.

Expression of Mer and Axl RTKs in astrocytoma patient samples and cell lines. A, microarray coexpression of Mer and Axl in astrocytomas, as measured by normalized hybridization intensity. B and C, immunoblot of Mer and Axl in patient samples with low-grade astrocytoma (LGA) and high-grade astrocytoma/glioma (HGG; B) and astrocytoma cell lines (C). Immunoblots are representative of three independent experiments and consist of a single membrane that was stripped and immunoblotted for individual proteins. Actin is shown as a protein loading control.

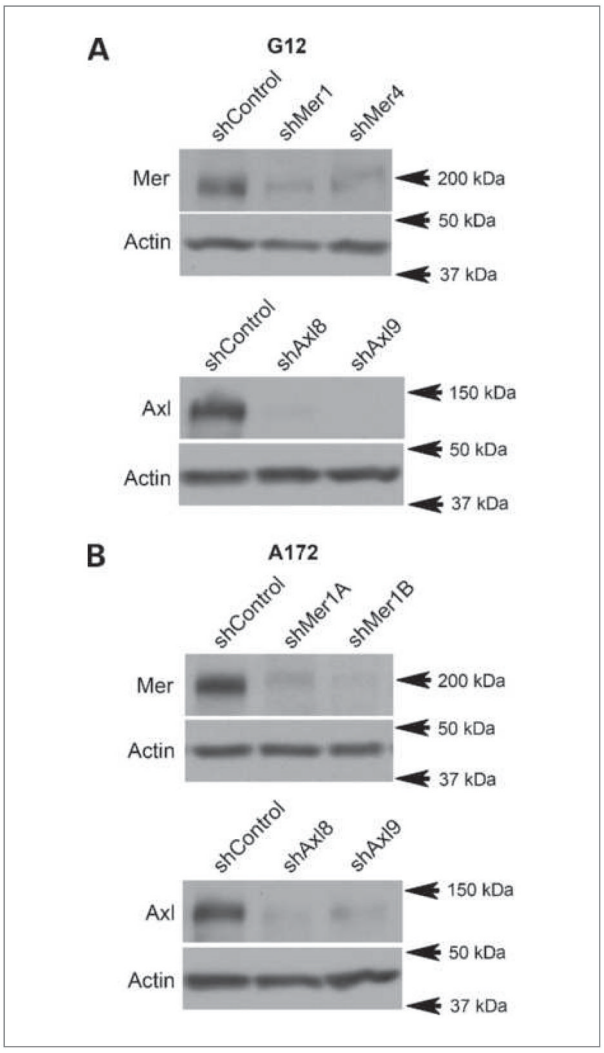

Figure 2.

Mer and Axl RTK protein expression following shRNA knockdown. A, immunoblot of Mer and Axl expression in the G12 astrocytoma line. shControl represents the parental line after transduction of shGFP, shMer1 and shMer4 represent independent constructs against Mer, whereas shAxl8 and shAxl9 represent independent constructs against Axl. Immunoblots are representative of three independent experiments and consist of a single membrane that was stripped and immunoblotted for individual proteins. Actin is shown as a protein loading control. B, immunoblot of Mer and Axl expression in the A172 astrocytoma line. shControl represents the parental line after transduction of shGFP, shMer1A and shMer1B are different lines derived from a single shRNA construct against Mer, whereas shAxl8 and shAxl9 represent independent shRNA constructs against Axl. Immunoblots are representative of three independent experiments. Actin is shown as a protein loading control.

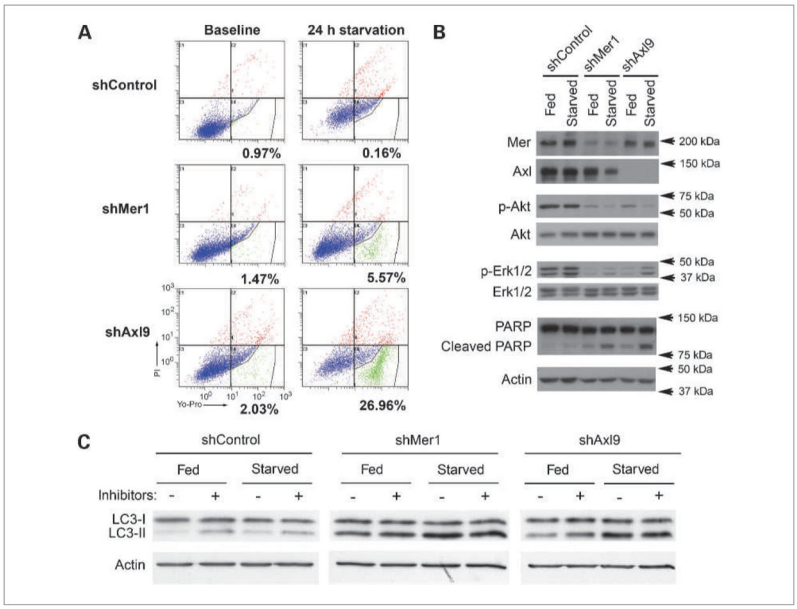

Figure 3.

Characterization of apoptotic and autophagic phenotype in G12 cells following knockdown of Mer or Axl expression. A, Yo-Pro/PI flow cytometric evaluation of G12 control line (shControl, top), shMer1 (middle), and shAxl9 (bottom) at baseline (left) and after 24 h of serum starvation (right). Percentages represent gated cells (green) that are undergoing early apoptosis. B, immunoblot of total Mer, total Axl, phosphorylated Akt (p-Akt), phosphorylated Erk1/2 (p-Erk1/2), and poly(ADP-ribose) polymerase (PARP) cleavage in the G12 control (shControl), shMer1, and shAxl9 lines at baseline (Fed) and after being serum starved (Starved) for 24 h. Total Akt, total Erk1/2, and actin are shown as protein loading controls. Immunoblots are representative of three independent experiments and consist of a single membrane that was stripped and immunoblotted for individual proteins. C, immunoblot of LC3-I and LC3-II of G12 control (shControl), shMer1, and shAxl9 lines at baseline (Fed) and after being serum starved (Starved) for 4 h, without (−) or with (+) the addition of lysosomal protease inhibitors pepstatin A and E64D. Representative immunoblots of three independent experiments. Actin is shown as a protein loading control.

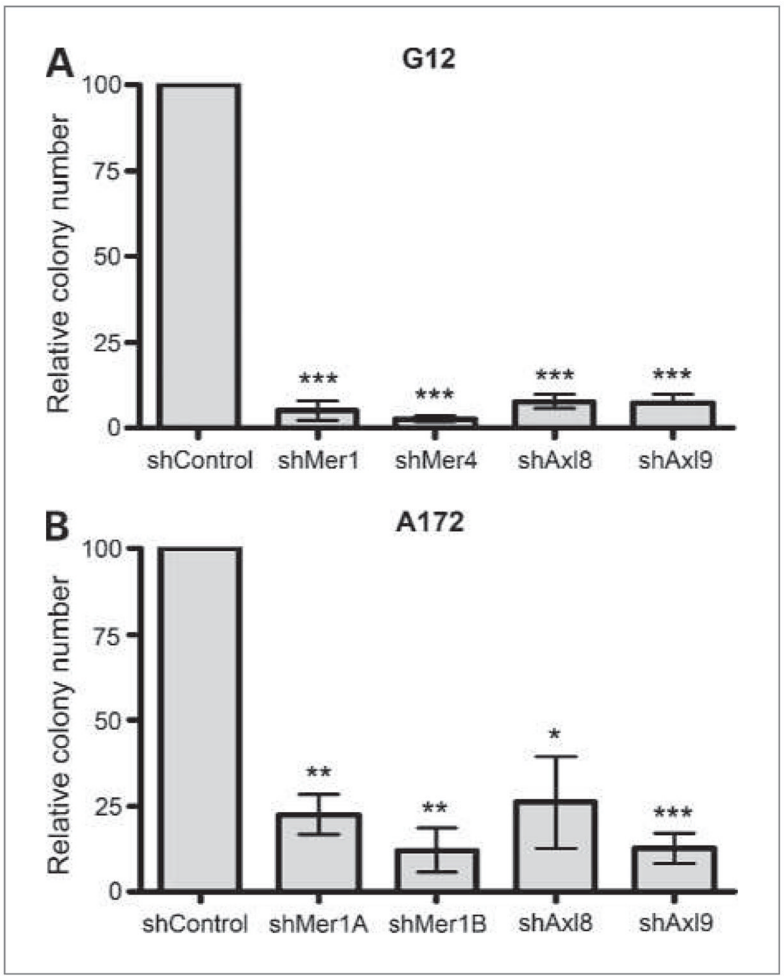

Figure 4.

Long-term soft-agar colony growth of astrocytoma cells. A, G12 knockdown cells were plated in soft agar and colonies were counted 3 wk later. shControl represents the parental line after transduction of shGFP, shMer1 and shMer4 represent independent constructs against Mer, whereas shAxl8 and shAxl9 represent independent constructs against Axl. ***, $P < 0.005$, in comparison to the control (two-tailed *t* test). Error bars represent three independent experiments that were done in triplicate. B, A172 knockdown cells were plated in soft agar and colonies were counted 3 wk later. shControl represents the parental line after transduction of shGFP, shMer1A and shMer1B are different lines derived from a single shRNA construct against Mer, whereas shAxl8 and shAxl9 represent independent constructs against Axl. *, $P < 0.05$; **, $P < 0.01$; ***, $P < 0.005$, in comparison to the control (two-tailed *t* test). Error bars represent three independent experiments that were done in triplicate.

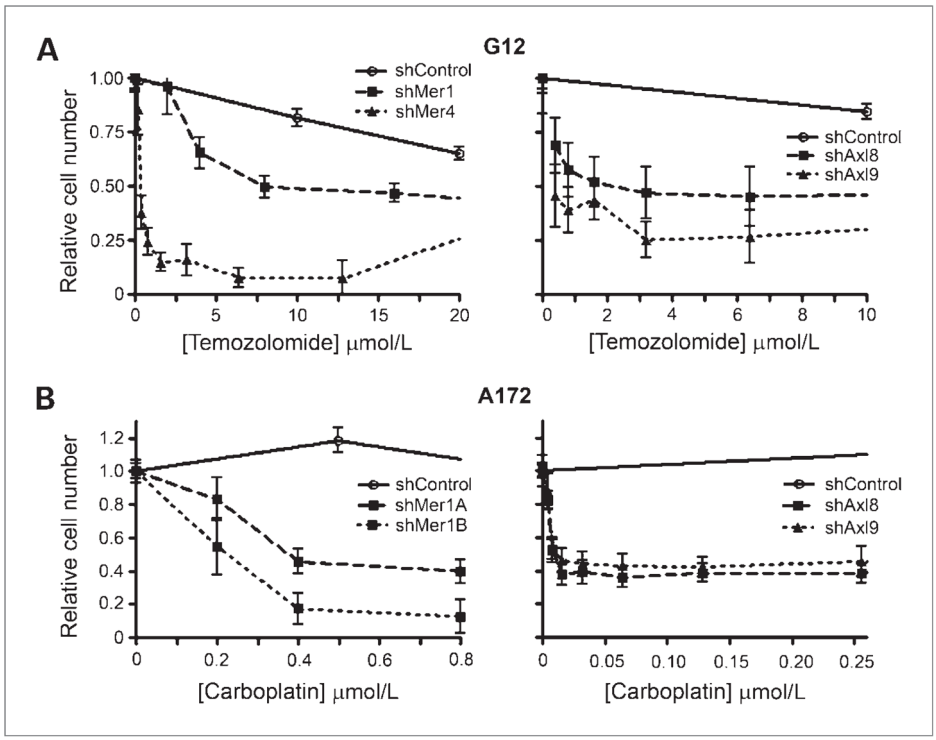

Figure 5.

Chemosensitivity of astrocytoma cells as evaluated by MTT assay. A, G12 control (shControl) and knockdown cells (shMer1 and shMer4; shAxl8 and shAxl9) were plated in 96-well plates at concentrations determined to allow linear growth over 3 d. Cells were treated with varying concentrations of temozolomide and relative cell number was assessed 48 h after treatment by colorimetric assessment/MTT assay. Error bars represent three independent experiments that were done in triplicate. B, A172 control (shControl) and knockdown cells (shMer1A and shMer1B; shAxl8 and shAxl9) were plated in 96-well plates at concentrations determined to allow linear growth over 3 d. Cells were treated with varying concentrations of carboplatin and relative cell number was assessed 48 h after treatment by colorimetric assessment/MTT assay. Error bars represent three independent experiments that were done in triplicate.

Mol Cancer Ther. Author manuscript; available in PMC 2011 July 18.

Table 1

The IC_{50} with 95% CI for G12 and A172 control and Mer and Axl knockdown cells in response to chemotherapy

	Temozolomide (μmol/L)		Carboplatin (μmol/L)		Vincristine (nmol/L)	
	IC_{50} (95% CI)	**P< 0.05**	**IC_{50} (95% CI)**	**P< 0.05**	**IC_{50} (95% CI)**	**P< 0.05**
G12						
shControl	68.6 (59.5–79.1)		47.9 (29.48–77.98)		1.64 (1.36–1.98)	
shMer1	18.2 (11.7–28.3)	*	0.78 (0.27–2.26)	*	0.74 (0.62–0.88)	*
shMer4	1 (0.52–1.91)	*	0.19 (0.14–0.25)	*	0.22 (0.17–0.30)	*
shAxl8	6.9 (2.30–20.84)	*	0.28 (0.03–4.83)	*	0.31 (0.23–0.44)	*
shAxl9	1.8 (0.61–5.36)	*	0.2 (IND)	NS	0.2 (0.12–0.33)	*
A172						
shControl	51.4 (40.6–65.0)		NR		2.54 (1.91–3.37)	
shMer1A	21.3 (15.0–30.0)	*	0.82 (0.36–1.80)	*	1.25 (0.96–1.63)	*
shMer1B	7.7 (5.5–10.7)	*	0.21 (0.13–0.35)	*	0.54 (0.42–0.66)	*
shAxl8	27.6 (19.3–39.5)	*	0.035 (0.02–0.08)	*	0.68 (0.53–0.86)	*
shAxl9	38.9 (26.6–56.6)	NS	0.075 (0.03–0.19)	*	2.92 (1.89–4.51)	NS

NOTE: “NR” indicates an IC_{50} was never reached. “IND” represents that the CI was indeterminate. The IC_{50} for each knockdown line was compared with the control line;

* indicates that the comparison is statistically different whereas an “NS” represents that there was no statistically significant difference because either the CI was indeterminate (as with the G12 shAxl9 line treated with carboplatin) or it overlapped with the shControl CI.